Одержано аналітичний зв'язок часу виходу термоелектричного охолоджувача на стаціонарний режим у залежності від термоелектричних параметрів конструкторських і технологічних елементів, перепаду температур, відносних робочих струмів, електричних опорів і геометричних параметрів термоелементів.

Проведено аналіз математичної моделі відносно часових і надійністних показників для різноманітних струмових режимів роботи і перепадів температури з урахуванням енергетичних показників і конструктивних параметрів термоелектричного охолоджувача.

Показано, що при зростанні часу виходу на стаціонарний режим для різних перепадів температур зменшується робочий струм, а функціональна залежність холодильного коефіцієнту від часу виходу на стаціонарний режим має максимум, якій залежить від перепаду температур. При заданому часі виходу на стаціонарний режим залежність кількості термоелементів від перепаду температур має мінімум. При зростанні часу виходу на постійний режим зменшується відносна інтенсивність відмов і зростає вірогідність безвідмовної роботи термоелектричного охолоджувача. З ростом перепаду температур для різних струмових режимів зростає час виходу на стаціонарний режим, зростає величина робочого струму, зменшується холодильний коефіцієнт, зростає кількість термоелементів і інтенсивність відмов.

Представлено розрахунок охолоджувача з заданим часом виходу на стаціонарний режим при заданих перепадах температур, зовнішніх умовах, тепловому навантаженні, геометрії гілок термоелементів. Одержані результати досліджень дозволяють проектувати однокаскадні термоелектричні охолоджувачі з заданою динамікою функціонування і прогнозувати основні параметри і показники надійності на любому часовому відрізці

Ключові слова: термоелектричний охолоджувач, час виходу на режим, показники надійності, режими роботи

UDC 621.362.192
DOI: 10.15587/1729-4061.2019.184400

DESIGNING A SINGLE-CASCADE THERMOELECTRIC COOLER WITH THE PREDEFINED TIME TO ENTER A STATIONARY MODE OF OPERATION

V. Zaykov
PhD, Head of Sector
Research Institute «STORM»
Tereshkovoi str., 27, Odessa, Ukraine, 65076
E-mail: gradan@i.ua

V. Mescheryakov
Doctor of Technical Sciences, Professor,
Head of Department
Department of Informatics
Odessa State Environmental University
Lvivska str., 15, Odessa, Ukraine, 65016
E-mail: gradan@ua.fm

Yu. Zhuravlov
PhD, Associate Professor
Department of Technology of
Materials and Ship Repair
National University «Odessa Maritime Academy»
Didrikhsona str., 8, Odessa, Ukraine, 65029
E-mail: ivanovich1zh@gmail.com

Received date 17.08.2019
Accepted date 15.11.2019
Published date 23.12.2019

1. Introduction

When designing thermoelectric cooling devices (TCD) for the heat-loaded elements of electronics operating under pulsed, short-term, and cyclical modes, the main requirement is to ensure a predetermined thermal mode of operation in real time. Going beyond the boundary temperature limits leads to failure not only of a given element, but, often, of the entire control system.

When constructing a thermoelectric cooler, the following is usually set: temperature difference ΔT, temperature of a heat-emitting joint T=300 K, heat load magnitude Q_0. Various limitations are imposed: on power consumption W, on working current magnitude I, on reliability indicators: failure rate λ and failure-free operation probability P.

The conditions for thermoelectric cooler operation in terms of specific operating conditions impose requirements on its dynamic characteristics and, contrary to them, indicators of reliability. Finding a compromise in the design of coolers is a relevant task of our study.

2. Literature review and problem statement

The results of thermodynamic studies into the systems that ensure the thermal modes of microprocessor elements built on thermoelectric devices are reported in work [1]. It has been shown that an increase in the density of thermal flows leads to a deterioration in the reliability of coolers. Paper [2] describes studies of the connection between a heat load and the mechanical deformation of thermoelectric materials, which cannot be compensated by free deformation. Article [3] addresses analysis of the effect of a temperature gradient on the mechanical stresses and the related reliability of thermoelectric coolers. Given the fundamental character of a reliability concept, studies on the impact of

various factors on reliability indicators are quite common in the scientific literature. An effect of the temperature and heat stress around an elliptical functional defect in a thermoelectric material was considered in [4]. A solution to this problem was a devised technique to improve the structural integrity of thermoelectric modules with changing geometry [5], which reduced the impact of thermal deformations. The results from studying the effect of heterogeneous thermal fields emerging in the heterogeneities of a thermoelectric material and macro-scale holes on reliability indicators of the cooler are reported in [6]. Authors of [7] presented a numerical simulation of the thermoelectric cooler taking into consideration the circulation of heat in the air gaps between the thermoelements, which affect their temperature gradients. Work [8] considers the impulse operation of thermoelectric coolers, which leads to an increase in average cooling capacity, but the pulse mode exacerbates the problem of temperature gradients.

The studies on the impact of heat flow density, mechanical deformation due to a temperature gradient, structural integrity of a thermoelectric material, on the TCD reliability are qualitative in character and do not make it possible to numerically assess and predict reliability indicators.

The needs of aerospace applications have made reliability indicators prioritized in the development of thermoelectric devices using a topology optimization [9]. However, mechanical stresses are only one component of the reliability problem. Another aspect related to the problem of reliability of thermoelectric coolers is the pulse operation of thermoelectric coolers [10], at which a change in temperature gradients becomes an operational mode of the cooler. Switch mode is used for accelerated testing of thermoelectric coolers, under which operational reliability indicators deteriorate by an order of magnitude. The need to use a pulse mode as a working one in the systems of maintaining operational conditions for heat-loaded elements suggests that research is needed on the ability to manage the dynamic characteristics of thermoelectric coolers [11]. An analysis of the relationship between the dynamics and reliability indicators of the cooler and its structure and modes of operation is given in [12]. A study [13] was carried out into the time it takes to enter a stationary mode, taking into consideration the influence of mass and technological elements in a single-cascade thermoelectric device. The dynamics and reliability indicators for the thermoelectric cooler with a certain geometry of branches were analyzed in [14] producing optimized solutions.

At the same time, when designing TCDs for the elements of electronics that function under stationary, especially pulse, short-term, and cyclical modes, the main requirement is to ensure the predetermined thermal mode of operation in real time.

3. The aim and objectives of the study

The aim of this study is to determine the attainable time it takes for a single-cascade thermoelectric cooler to enter a stationary mode of operation in a predefined range of temperature changes and working currents.

To accomplish the aim, the following tasks have been set:

– to analyze a dynamic model of TCD in the range of working temperature changes under the main energy modes of a single-cascade cooler's operation;

– by setting the time it takes to enter a stationary mode, determine the required relative working current, basic energy indicators, the number of thermoelements and the intensity of failures.

4. Dynamic model of a thermoelectric cooler in the range of working temperature changes and working currents

Based on the analysis of ratios given in [11], we derived an expression to determine a relative working current B_K, depending on the time it takes to enter a stationary mode of operation τ

$$B_K^2 - 2B_K \frac{A-\gamma B_H}{A-\gamma B_H^2} + \frac{A\Theta}{A-\gamma B_H^2} = 0, \quad \sqrt{a^2+b^2}, \tag{1}$$

where

$$A = \exp \frac{\tau K\left(1+2B_K \frac{\Delta T_{\max}}{T_0}\right)}{\sum_i m_i C_i};$$

$B_H = I_{\max K}/I_{\max H}$.

By solving equation (1), we obtain

$$B_K = \left(\frac{A-\gamma B_H}{A-\gamma B_H}\right)\left[1-\sqrt{1-\frac{A\Theta\left(A-\gamma B_H\right)}{\left(A-\gamma B_H\right)}}\right]. \tag{2}$$

The minimum time it takes to enter a stationary mode of operation $\tau_{\min}$ is ensured under a $Q_{0\max}$ mode (at B_K=1)

$$\tau_{\min} = \frac{\sum_i m_i C_i}{K\left(1+2\frac{\Delta T_{\max}}{T_0}\right)} \ln \frac{\gamma B_H\left(2-B_H\right)}{1-\Theta}, \tag{3}$$

where:

– $\sum_i m_i C_i = 175\times 10^{-4}$ J/K – the total magnitude of the product of heat intensity and the mass of CTE components at l/S=10 cm^{-1};

– $B_K = I/I_{\max K}$ – relative working current at τ;

– I – magnitude of the working current, A;

– $I_{\max K} = e_K T_0/R_K$ – maximal working current, A;

– $I_{\max K}$, R_K – maximal working current, A, and electrical resistance of a thermoelement branch, Ohm, at the end of a cooling process, respectively;

– T_0 – temperature of a heat-absorbing joint, K, at τ_K;

– $K = \overline{\varkappa}_K/(l/S)$ – heat transfer ratio, W/K;

– $\overline{\varkappa}_K$ – average thermal conductivity ratio of thermoelectric materials, W/(cm·K);

– l/S – height l and cross-sectional area S of a thermoelement's branch, 1/cm, respectively;

– $\gamma = \frac{I_{\max H}^2 R_H}{I_{\max K}^2 R_K}$;

– $I_{\max H} = e_H T/R_H$ – maximum working current, A, at τ=0;

– $I_{\max H}$, R_H – maximum working current, A, and electrical resistance of a thermoelement's branch, Ohm, respectively, at the beginning of a cooling process at τ=0;

– e_H, e_K – thermoEMF ratio of a thermoelement's branch at the beginning and end of the cooling process, V/K, respectively;

– T – heat-absorbing joint's temperature at the beginning of the cooling process, K;

– $B_H=I/I_{\max H}$ – relative working current at $\tau=0$;

– $\Theta=\Delta T/T_{\max}$ – relative temperature difference;

– $\Delta T=T-T_0$ – working temperature difference, K;

– $\Delta T_{max}=0.5\overline{z}T_0^2$ – maximum temperature difference, K;

– $\overline{z}$ – averaged efficiency of a thermoelectric material in the module, 1/K.

A TCD's power consumption W_K can be determined from expression:

$$W_K=2nI_{\max K}^2R_KB_K\left(B_K+\frac{\Delta T_{\max}}{T_0}\Theta\right), \quad (4)$$

where n is the number of thermoelements, pieces.

The number of thermoelements n can be determined from expression

$$n=\frac{Q_0}{I_{\max K}^2R_K\left(2B_K-B_K^2-\Theta\right)}, \quad (5)$$

where Q_0 is the magnitude of a heat load, W.

Voltage drop is

$$U_K=W_K/I. \quad (6)$$

The refrigeration factor E can be defined from expression

$$E=Q_0/W_K. \quad (7)$$

The relative magnitude of failure intensity λ/λ_0 can be determined from formula [15]

$$\lambda/\lambda_0=nB_K^2(\Theta+C)\frac{\left(B_K+\frac{\Delta T_{\max}}{T_0}\Theta\right)^2}{\left(1+\frac{\Delta T_{\max}}{T_0}\Theta\right)^2}K_T, \quad (8)$$

where $C=\frac{Q_0}{I_{\max K}^2R_Kn}$ is the relative heat load; K_T is the factor of lower temperatures [15].

The probability of failure-free operation P can be determined from expression

$$P=\exp(-\lambda t), \quad (9)$$

where t is the assigned resource, hours.

5. Analysis of the model's time and reliability indicators for different current modes and temperature changes

Let us set the time that it would take to enter a stationary mode of operation τ, taking into consideration CTE at the assigned temperature difference ΔT and heat load Q_0. By using a method of sequential approximations, one can determine a relative working current B_K and, therefore, the basic parameters and reliability indicators. One or two approximations would suffice.

Table 1 gives the results of calculations, relative to working current B_K, of basic parameters, reliability indicators, for temperature changes ΔT=20; 30, 40; 50; 60 K at heat load Q_0=0.5 W, when $l/S=10$ cm^{-1}, considering

$$\sum_i m_iC_i=175\times10^{-4}\ \text{J/K}.$$

Table 1

Results of calculating the basic parameters and indicators of TCD

τ, s	B_K	I, A	n, pcs.	W, W	E	U, V	B_H	λ/λ_0	$\lambda\cdot10^8$, 1/h	P	Mode of operation
1	2	3	4	5	6	7	8	9	10	11	12
ΔT=20 K; T=300 K; $\Delta T_{\max}$=93.7 K; Θ=0.213; $K=15.8\cdot10^{-4}$ W/K; γ=1.132; $R_K=10.64\cdot10^{-3}$ Ohm; $I_{\max K}$=5.29 A											
2.4	1.0	5.29	2.1	1.34	0.373	0.25	0.96	2.12	6.37	0.99936	$Q_{0\max}$
3.8	0.46	2.44	3.4	0.50	1.0	0.20	0.44	0.128	0.38	0.999962	$(Q_0/I)_{\max}$
4.0	0.44	2.32	3.6	0.48	1.05	0.21	0.421	0.107	0.32	0.999968	–
5.0	0.35	1.84	4.7	0.41	1.23	0.22	0.333	0.05	0.15	0.999985	–
6.0	0.29	1.55	5.9	0.37	1.33	0.24	0.281	0.03	0.09	0.9999912	–
7.0	0.26	1.35	7.2	0.356	1.40	0.26	0.245	0.02	0.06	0.9999942	–
8.8	0.213	1.13	10.0	0.36	1.40	0.32	0.204	0.012	0.036	0.9999963	$(Q_0/I^2)_{\max}$
14.1	0.158	0.84	21.5	0.46	1.08	0.55	0.152	0.0072	0.022	0.9999979	$\lambda_{\min}$
ΔT=30 K; T=300 K; $\Delta T_{\max}$=86.8 K; Θ=0.346; $K=15.8\cdot10^{-4}$ W/K; γ=1.23; $R_K=10.3\cdot10^{-3}$ Ohm; $I_{\max K}$=5.16 A											
4.2	1.0	5.16	2.8	1.71	0.29	0.33	0.94	2.84	8.5	0.99915	$Q_{0\max}$
5.7	0.588	3.0	3.8	0.86	0.58	0.28	0.55	0.43	1.30	0.99987	$(Q_0/I)_{\max}$
7.0	0.466	2.4	4.9	0.72	0.69	0.30	0.436	0.21	0.63	0.999937	–
9.8	0.346	1.8	8.0	0.69	0.72	0.39	0.32	0.095	0.28	0.999972	$(Q_0/I^2)_{\max}$
12	0.30	1.55	11.1	0.75	0.67	0.48	0.28	0.071	0.213	0.999978	–
14.5	0.266	1.37	15.8	0.87	0.58	0.63	0.25	0.06	0.18	0.999982	$\lambda_{\min}$
ΔT=40 K; T=300 K; $\Delta T_{\max}$=86.8 K; Θ=0.50; $K=16.0\cdot10^{-4}$ W/K; γ=1.324; $R_K=10.1\cdot10^{-3}$ Ohm; $I_{\max K}$=5.02 A											
6.5	1.0	5.02	3.9	2.31	0.216	0.46	0.911	3.8	11.4	0.9989	$Q_{0\max}$

Continuation of Table 1

1	2	3	4	5	6	7	8	9	10	11	12
7.8	0.71	3.55	4.7	1.46	0.342	0.41	0.644	1.23	3.7	0.99963	$(Q_0/I)_{max}$
11.0	0.50	2.5	7.9	1.32	0.38	0.52	0.456	0.49	1.46	0.99985	$(Q_0/I^2)_{max}$
15.1	0.40	2.0	14.0	1.58	0.32	0.79	0.364	0.34	1.0	0.99990	λ_{min}
ΔT=50 K; T=300 K; ΔT_{max}=73.1 K; Θ=0.684; K=16.0·10^{-4} W/K; γ=1.434; R_K=9.4·10^{-3} Ohm; I_{maxK}=5.0 A;											
10.4	1.0	5.0	6.7	3.8	0.13	0.77	0.91	6.9	20.7	0.9979	Q_{0max}
11.4	0.82	4.1	7.4	2.95	0.170	0.73	0.75	3.7	11.1	0.9989	$(Q_0/I)_{max}$
13.6	0.684	3.42	9.85	2.79	0.179	0.82	0.62	2.3	6.9	0.99931	$(Q_0/I^2)_{max}$
15	0.630	3.15	11.9	2.92	0.171	0.93	0.57	2.0	6.0	0.99940	–
17	0.58	2.90	15.2	3.23	0.155	1.11	0.526	1.83	5.48	0.99945	λ_{min}
ΔT=60 K; T=300 K; ΔT_{max}=66.8 K; Θ=0.898; K=16.2·10^{-4} W/K; γ=1.547; R_K=9.26·10^{-3} Ohm; I_{maxK}=4.85 A											
18.7	1.0	4.85	22.5	12.3	0.041	2.50	0.88	23.3	70.0	0.9930	Q_{0max}
19.2	0.948	4.60	23.2	11.49	0.0435	2.50	0.834	19.77	59.3	0.99405	$(Q_0/I)_{max}$
20.0	0.898	4.36	25.0	11.2	0.0445	2.58	0.79	17.4	52.2	0.9948	$(Q_0/I^2)_{max}$
22.2	0.835	4.05	30.6	12.1	0.0414	3.0	0.735	16.2	48.6	0.9952	λ_{min}

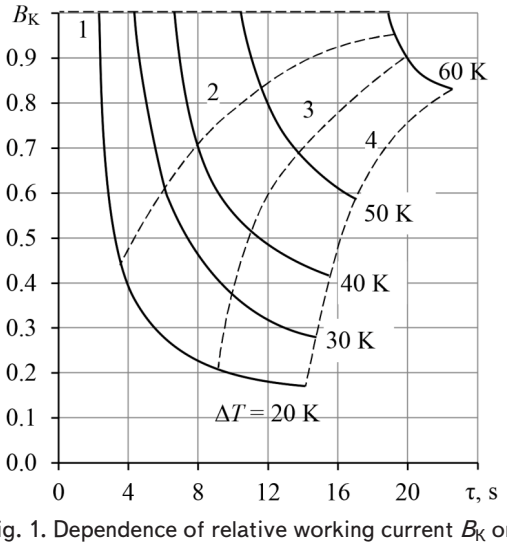

Fig. 1. Dependence of relative working current B_K on the time it takes to enter a stationary mode τ for a single-cascade TCD at T=300 K, I/S=10 cm^{-1}; Q_0=0.5 W at different temperature differentials ΔT for different modes of operation: 1 – Q_{0max} mode; 2 – $(Q_0/I)_{max}$ mode; 3 – $(Q_0/I^2)_{max}$ mode; 4 – λ_{min} mode

An increase in the time it takes to enter a stationary mode τ for different time differentials ΔT leads to the following:

– the relative working current B_K decreases, except for the Q_{0max} mode (Fig. 1), where the dotted line indicates characteristic current modes of operation. The magnitude of relative working current B_K is reduced from the Q_{0max} mode (pos. 1) to the λ_{min} mode (pos. 4). At the predefined time to enter a stationary mode τ, an increase in temperature difference ΔT increases the relative working current B_K;

– the magnitude of working current I decreases (Fig. 2), where the dotted line indicates the magnitude of a working current for the characteristic current modes of operation. The magnitude of the working current decreases from the Q_{0max} mode to the λ_{min} mode. At the predefined time to enter a stationary mode τ, an increase in temperature difference ΔT increases the magnitude of working current I;

– functional dependence $E=f(\tau)$ (Fig. 3) has a maximum: E_{max}=1.4 at ΔT=20 K; E_{max}=0.73 at ΔT=30 K; E_{max}=0.37 at ΔT=40 K; E_{max}=0.17 at ΔT=50 K; E_{max}=0.044 at ΔT=60 K. At the predefined time to enter a stationary mode τ, the refrigeration factor decreases as the temperature difference ΔT drops. The dotted line indicates the magnitude of the refrigeration factor for the characteristic current modes of operation;

– the number of thermoelements n increases (Fig. 4); the dotted line indicates the number of thermal elements for the characteristic current modes of operation; at the predefined time to enter a stationary mode τ, at increase in the temperature difference ΔT, functional dependence $n=f(\Delta T)$ has a minimum;

– functional dependence $U=f(\tau)$ (Fig. 5) has a minimum: U_{min}=0.2 V at ΔT=20 K; U_{min}=0.28 V at ΔT=30 K; U_{min}=0.41 V at ΔT=40 K; U_{min}=0.73 V at ΔT=50 K; U_{min}=2.5 V at ΔT=60 K. The dotted line indicates the magnitude of voltage drop for the characteristic current modes of operation. At the predefined time to enter a stationary mode τ, an increase in temperature difference ΔT increases the magnitude of the voltage drop;

– the relative magnitude of intensity of failures λ/λ_0 (Fig. 6) decreases. The dotted line indicates the relative failure rate for the characteristic current modes of operation. The magnitude of failure intensity λ decreases from the Q_{0max} mode (pos. 1) to the λ_{min} mode (pos. 4). At the predefined time to enter a stationary mode τ, an increase in temperature difference ΔT increased the relative magnitude of failure intensity λ/λ_0;

– the likelihood of failure-free operation P increases (Fig. 7). The dotted line indicates the probability of failure-free work for the characteristic current modes of operation. The probability of failure-free operation increases from the Q_{0max} mode (pos. 1) to the λ_{min} mode (pos. 4). At the predefined time to enter a stationary mode τ, an increase in temperature difference ΔT increases the probability of failure-free work P.

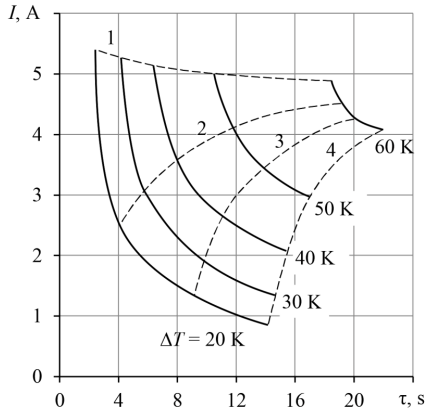

Fig. 2. Dependence of the magnitude of working current I on the time it takes to enter a stationary mode τ for a single-cascade TCD at T=300 K, I/S=10 cm^{-1}; Q_0=0.5 W at different temperature differentials ΔT for different modes of operation: 1 – Q_{0max} mode; 2 – $(Q_0/I)_{max}$ mode; 3 – $(Q_0/I^2)_{max}$ mode; 4 – λ_{min} mode

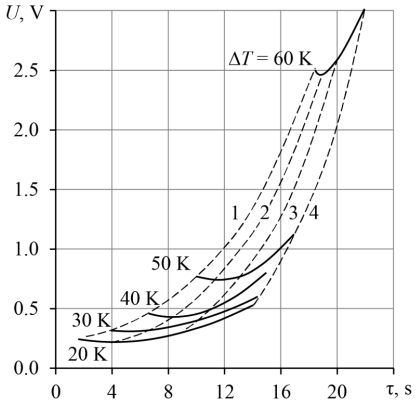

Fig. 5. Dependence of voltage drop U on the time to enter a stationary mode τ for a single-cascade TCD at T=300 K, I/S=10 cm^{-1}; Q_0=0.5 W, at different temperature differences ΔT, for different modes of operation: 1 – Q_{0max} mode; 2 – $(Q_0/I)_{max}$ mode; 3 – $(Q_0/I^2)_{max}$ mode; 4 – λ_{min} mode

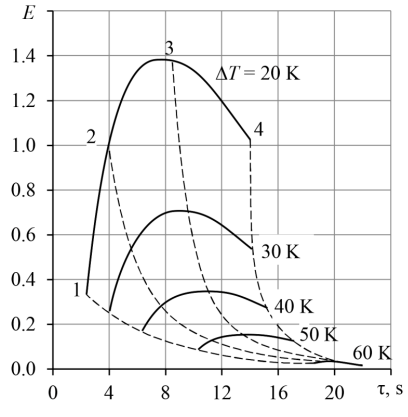

Fig. 3. Dependence of refrigeration factor E on the time it takes to enter a stationary mode τ for a single-cascade TCD at T=300 K, I/S=10 cm^{-1}; Q_0=0.5 W, at different temperature differences ΔT, under different modes of operation: 1 – Q_{0max} mode; 2 – $(Q_0/I)_{max}$ mode; 3 – $(Q_0/I^2)_{max}$ mode; 4 – λ_{min} mode

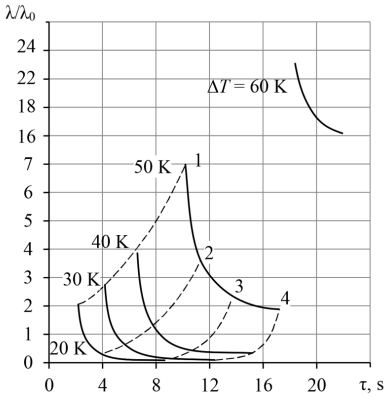

Fig. 6. Dependence of the relative magnitude of failure intensity λ/λ_0 on the time it takes to enter a stationary mode for a single-cascade TCD at T=300 K, I/S=10 cm^{-1}; Q_0=0.5 W; λ_0=3×10^{-9} 1/h at different temperature difference ΔT, for different modes of operation: 1 – Q_{0max} mode; 2 – $(Q_0/I)_{max}$ mode; 3 – $(Q_0/I^2)_{max}$ mode; 4 – λ_{min} mode

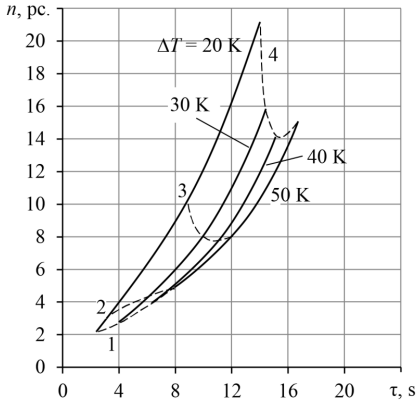

Fig. 4. Dependence of the number of thermo-elements n on the time to enter a stationary mode τ for a single-cascade TCD at T=300 K, I/S=10 cm^{-1}; Q_0=0.5 W at different temperature differences ΔT, for different modes of operation: 1 – Q_{0max} mode; 2 – $(Q_0/I)_{max}$ mode; 3 – $(Q_0/I^2)_{max}$ mode; 4 – λ_{min} mode

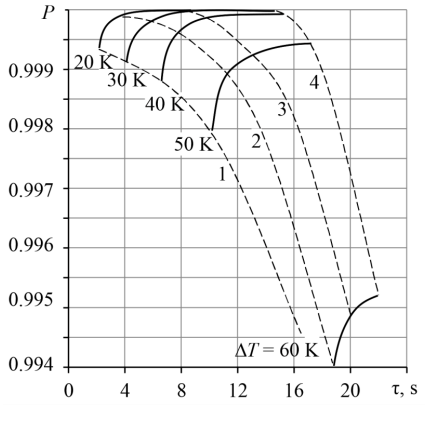

Fig. 7. Dependence of the probability of failure-free operation P on the time to enter a stationary mode τ for a single-cascade TCD at T=300 K, I/S=10 cm^{-1}; Q_0=0.5 W; t=10^{-4} h at different temperature difference ΔT for different modes of operation: 1 – Q_{0max} mode; 2 – $(Q_0/I)_{max}$ mode; 3 – $(Q_0/I^2)_{max}$ mode; 4 – λ_{min} mode

A growth in temperature difference ΔT for different current regimes leads to the following:

– the time it takes to enter a stationary mode τ increases (Fig. 8). At the assigned temperature difference ΔT, the time to enter a stationary mode increases from τ_{min}=6.5 s, in the Q_{0max} mode (pos. 1) to τ=15.1 s in the $\lambda_{min\ mode}$ (pos. 4). At temperature changes ΔT close to ΔT_{max}, the time to enter a stationary mode τ differs slightly;

– the magnitude of working current I increases (Fig. 9) for characteristic current modes $(Q_0/I)_{max}$, $(Q_0/I^2)_{max}$, λ_{min} (pos. 2, 3, 4), and, for the Q_{0max} mode (pos. 1), it decreases. At the assigned temperature difference ΔT, for example ΔT=40 K, the magnitude of working current I increases from I_{min}=2 A in the λ_{min} mode (pos. 4) to I=5.02 A in the Q_{0max} mode (pos. 1);

– the refrigeration factor E decreases (Fig. 10); at the predetermined temperature difference ΔT, for example ΔT==40 K, the refrigeration factor E increases from E_{min}=0.216 in the Q_{0max} mode (pos. 1) to E=0.38 in the $(Q_0/I^2)_{max}$ mode (pos. 3);

– the number of thermo-elements n (Fig. 11) for the Q_{0max} mode (pos. 1) and for the $(Q_0/I)_{max}$ mode increases (pos. 2). Functional dependence $n=f(\Delta T)$ (Fig. 5) has a minimum for the $(Q_0/I^2)_{max}$ mode (pos. 3) at ΔT=40 K and for the λ_{min} mode (pos. 4) at ΔT=40 K. At the assigned temperature difference ΔT, for example ΔT=40 K, the number of thermal elements n increases from n=3.9 pieces in the Q_{0max} mode (pos. 1) to n=14 pieces in the λ_{min} mode (pos. 4);

– the voltage drop U increases (Fig. 12). At the predefined temperature difference ΔT, for example, for temperature difference ΔT=40 K, the drop in voltage U increases from U=0.46 V in the $(Q_0/I)_{max}$ mode (pos. 2) to U=0.79 in the λ_{min} mode (pos. 4);

– the intensity of failures λ increases (Fig. 13); at the predefined temperature difference ΔT, for example ΔT=40 K, the relative magnitude of failure intensity λ/λ_0 decreases from $\lambda/\lambda_{0=}$3.8 in the Q_{0max} mode (pos. 1) to λ/λ_0=0.34 in the λ_{min} mode (pos. 4);

– the likelihood of failure-free operation P decreases (Fig. 14); at the predefined temperature difference ΔT, for example ΔT=40 K, the probability of failure-free operation P increases from P=0.9989 in the Q_{0max} mode (pos. 1) to P=0.99990 in the λ_{min} mode (pos. 4).

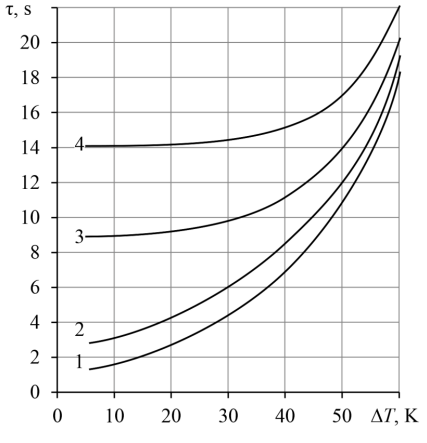

Fig. 8. Dependence of the time it takes to enter a stationary mode for a single-cascade TCD on temperature difference ΔT at T=300 K, l/S=10 cm^{-1}; Q_0=0.5 W for different modes of operation: 1 – Q_{0max}; 2 – $(Q_0/I)_{max}$; 3 – $(Q_0/I^2)_{max}$; 4 – λ_{min}

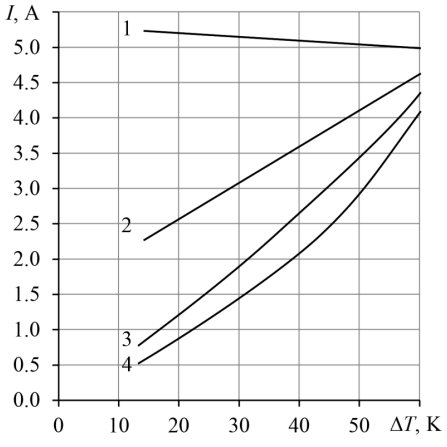

Fig. 9. Dependence of the magnitude of working current I for a single-cascade TCD on temperature difference ΔT at T=300 K, l/S=10 cm^{-1}; Q_0=0.5 W for different modes of operation: 1 – Q_{0max}; 2 – $(Q_0/I)_{max}$; 3 – $(Q_0/I^2)_{max}$; 4 – λ_{min}

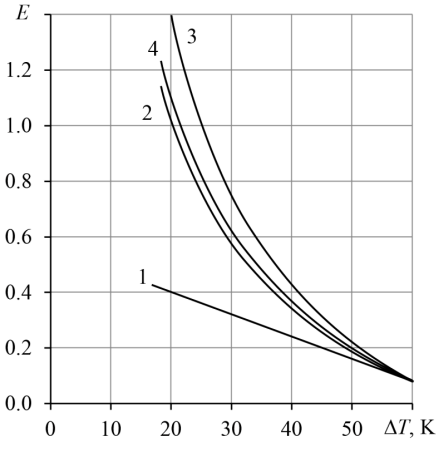

Fig. 10. Dependence of refrigeration factor E for a single-cascade TCD on temperature difference ΔT at T=300 K, l/S=10 cm^{-1}; Q_0=0.5 W for different modes of operation: 1 – Q_{0max}; 2 – $(Q_0/I)_{max}$; 3 – $(Q_0/I^2)_{max}$; 4 – λ_{min}

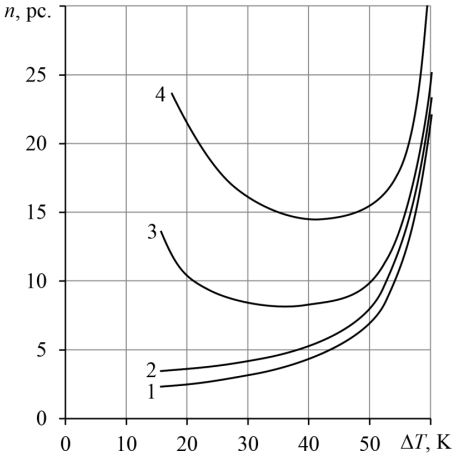

Fig. 11. Dependence of the number of thermo-elements n for a single-cascade TCD on temperature difference ΔT at T=300 K, l/S=10 cm^{-1}; Q_0=0.5 W for different modes of operation: 1 – Q_{0max}; 2 – $(Q_0/I)_{max}$; 3 – $(Q_0/I^2)_{max}$; 4 – λ_{min}

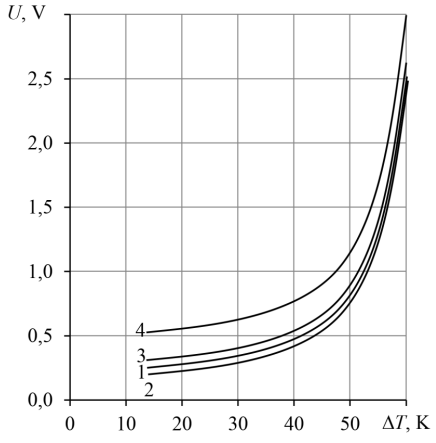

Fig. 12. Dependence of voltage drop U for a single-cascade TCD on temperature difference ΔT at T=300 K, l/S=10 cm^{-1}; Q_0=0.5 W for different modes of operation: 1 – Q_{0max}; 2 – $(Q_0/l)_{max}$; 3 – $(Q_0/l^2)_{max}$; 4 – λ_{min}

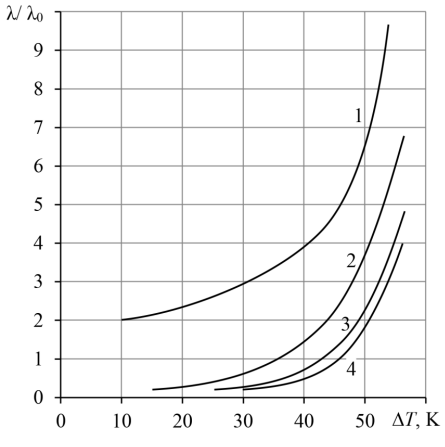

Fig. 13. Dependence of the relative magnitude of failure intensity for a single-cascade TCD on temperature difference ΔT at T=300 K, l/S=10 cm^{-1}; Q_0=0.5 W; λ_0=3×10^{-8} 1/h for different modes of operation: 1 – Q_{0max}; 2 – $(Q_0/l)_{max}$; 3 – $(Q_0/l^2)_{max}$; 4 – λ_{min}

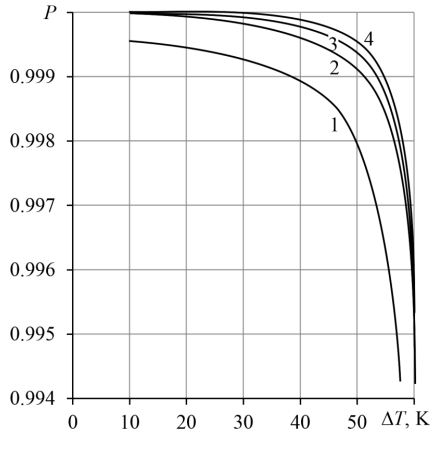

Fig. 14. Dependence of the probability of failure-free operation for a single-cascade TCD on temperature difference ΔT at T=300 K, l/S=10 cm^{-1}; Q_0=0.5 W; t=10^4 for different modes of operation: 1 – Q_{0max}; 2 – $(Q_0/l)_{max}$; 3 – $(Q_0/l^2)_{max}$; 4 – λ_{min}

Example of calculation.

Initial data: it is required to build a single-cascade thermoelectric cooler for temperature difference ΔT=40 K at T=300 K under heat load Q_0=0.5 W, the geometry of thermo-elements' branches l/S=10 cm^{-1} and the time to enter a stationary mode $\tau \leq 10$ s.

To build a TCD, we shall use the temperature dependences for the parameters of thermoelectric materials in module [15]. We shall determine in the initial period τ=0 T_0=T=300 K the electrical resistance of a thermoelement's branch and the maximum working current R_H=11.1·10^{-3}; I_{maxH}=5.51 A. Thus, at temperature difference ΔT=40 K , the average temperature is equal to

$$\overline{T} = \frac{T + T_0}{2} = 280 \text{ K};$$

$$\overline{z} = 2.36 \cdot 10^{-3}\, 1/\text{K}; \quad \overline{e} = 1.95 \cdot 10^{-4} \text{ V/K};$$

$$\overline{\sigma} = 990 \text{ S/cm};$$

$$\overline{æ} = 16.0 \cdot 10^{-3} \text{ W} / (\text{cm} \times \text{K}).$$

Define the basic parameters at ΔT=40 K:

R_K=10/990=10.1·10^{-3} Ohm;

I_{maxK}=5.02 A; K=16·10^{-4} W/K; γ=1.324.

At l/S=10 cm^{-1} $\sum_i m_i C_i = 175 \cdot 10^{-4}$ J/K considering CTE

ΔT_{max}=79.8 K; Θ=0.50; $\Delta T_{max}/T_0$=0.31; D=0.911.

By using the method of successive approximations, we shall determine the relative working current B_K. From Fig. 1, take at the beginning: B_K=0.53. Then

$$A = \exp\frac{10.\cdot 16.0 \cdot 10^{-4}(1 + 20.53 \cdot 0.31)}{175 \cdot 10^{-4}} =$$

$$= \exp\frac{212.6}{175} = 3.37.$$

Next, determine B_K from formula (2).

$$B_K = \frac{A - \gamma D}{A - \gamma D^2}\left[1 - \sqrt{1 - \frac{A\Theta\left(A - \gamma D^2\right)}{\left(A - \gamma D\right)^2}}\right] =$$

$$= \frac{3.37 - 1.324 \cdot 0.911}{3.37 - 1.324 \cdot 0.83} \times$$

$$\times\left[1 \pm \sqrt{1 - \frac{3.37 \cdot 0.50(3.37 - 1.324 \cdot 0.83)}{(3.37 - 1.32 \cdot 0.911)^2}}\right] =$$

$$= \frac{2.164}{2.27}\left[1 \pm \sqrt{1 - \frac{3.825}{4.68}}\right] = 0.953(1 \pm 0.427) = 0.546.$$

Refine B_K=0.546. Then

$$A = \exp\frac{10.0 \cdot 16.0 \cdot 10^{-4}(1 + 20.546 \cdot 0.31)}{175 \cdot 10^{-4}} =$$

$$= \exp\frac{214.2}{175} = 3.40.$$

$$B_{\text{K}} = \frac{3.4-1.206}{3.4-1.1}\left[1\pm\sqrt{1-\frac{3.4\cdot 0.5(3.4-1.1)}{(3.4-1.206)^2}}\right]=$$

$$=\frac{2.194}{2.3}\left[1\pm\sqrt{1-\frac{3.91}{4.814}}\right]=0.954(1\pm 0.433)=0.54.$$

Determine the magnitude of working current I from ratio

$I=I_{\max K}\ B_K=I_{\max H}\ B_H=2.71$ A (Fig. 2).

Then determine $B_H=0.492$. Next, determine the number of thermoelements n from expression (4):

$$n=\frac{Q_0}{I^2_{\max K}R_K\left(2B_K-B_K^2-\Theta\right)}=6{,}8 \text{ pc. (Fig. 4).}$$

The power consumption W_K can be determined from expression (3)

$$W_K=2nI^2_{\max K}R_KB_K\left(B_K+\frac{\Delta T_{\max}}{T_0}\Theta\right)=1{,}3 \text{ W.}$$

The voltage drop can be determined from formula (5)

$U_K=W_K/I=0.48$ V (Fig. 5).

The refrigeration factor E will be defined from expression (6)

$E=Q_0/W_K=0.385$ (Fig. 3).

The relative magnitude of failure-free operation λ/λ_0 can be determined from formula (7)

$$\lambda/\lambda_0=nB_K^2(\Theta+C)\times$$

$$\times\frac{\left(B_K+\frac{\Delta T_{\max}}{T_0}\Theta\right)^2}{\left(1+\frac{\Delta T_{\max}}{T_0}\Theta\right)^2}K_T=0.579, \text{ (Fig. 6).}$$

$\lambda=1.74\cdot 10^{-8}$ 1/h is the failure rate.

The probability of failure-free operation P is determined from formula (8) $P=0.99983$, which corresponds to the model studies described above (Fig. 7).

6. Discussion of results of analyzing the time it takes to enter a stationary mode for a single-cascade TCD

The results obtained are based on the devised model of a single-cascade thermoelectric cooling device for the assigned transition dynamics. The study was conducted in the range from 20 to 60 K at the typical heat load values $Q_0=0.5$ W for $l/S=10$ cm^{-1} and different characteristic current modes of operation.

Special feature of the proposed model, compared to existing models, is taking into consideration the impact of structural and technological elements on the dynamic characteristics and reliability indicators of the cooler.

Our analysis of results from calculating the main parameters and reliability indicators has revealed that an increase in the time to enter a stationary mode of operation τ leads, for varying temperature difference ΔT, to that:

1) the following reduces:

– relative working current B_K (Fig. 1). The minimum relative working current $B_K=0.4$ is ensured in the $\lambda_{\min}$ mode at temperature difference $\Delta T=40$ K and $\tau=16$ s;

– the magnitude of working current I (Fig. 2). The minimum magnitude of working current $I_{\min}=2$ A is ensured in the $\lambda_{\min}$ mode at $\Delta T=40$ K and $\tau=16$ s;

– the relative magnitude of intensity of failures λ/λ_0 (Fig. 6). The minimum relative failure rate $(\lambda/\lambda_0)_{\min}$ is ensured in the $\lambda_{\min}$ mode at $\Delta T=40$ K and $\tau=16$ s;

2) the following increases:

– the number of thermo-elements n (Fig. 4). The minimum quantity of thermoelements $n_{\min}=4$ pieces is ensured in the $Q_{0\max}$ mode at $\Delta T=40$ K;

– voltage drop U (Fig. 5). The maximum voltage drop $U_{\max}=1.0$ is ensured in the $\lambda_{\min}$ mode at $\Delta T=40$ K;

– the probability of failure-free operation P (Fig. 7). The maximum probability of failure-free operation $P_{\max}=0.99990$ is ensured at $\Delta T=40$ K.

Functional dependence of the refrigeration factor $E=f(\tau)$ has a maximum $E_{\max}=0.35$ at $\Delta T=40$ K (Fig. 3).

As the temperature drop ΔT increases, for different current modes of operation:

1) the following increases:

– the time it takes to enter a stationary mode of operation τ (Fig. 8). The minimum time to enter a stationary mode of operation $\tau_{\min}=7$ s at $\Delta T=40$ K is ensured in the $Q_{0\max}$ mode;

– the magnitude of working current I (Fig. 9). The minimum magnitude of working current $I_{\min}=2.0$ A is ensured in the $\lambda_{\min}$ mode at $\Delta T=40$ K and $\tau=16$ s;

– voltage drop U (Fig. 12). The maximum voltage drop $U_{\max}=0.75$ V is ensured in the $\lambda_{\min}$ mode at $\Delta T=40$ K;

– the relative failure rate λ/λ_0 (Fig. 13). The minimum failure intensity $(\lambda/\lambda_0)_{\min}=0.5$ is ensured in the $\lambda_{\min}$ mode at $\Delta T=40$ K;

2) the following decreases:

– refrigeration factor E (Fig. 10). The maximum refrigeration factor $E_{\max}=0.42$ is ensured at $\Delta T=40$ K;

– the probability of failure-free operation P (Fig. 14). The maximum probability of failure-free operation $P_{\max}=0.99990$ is ensured in the $\lambda_{\min}$ mode at $\Delta T=40$ K.

A limitation of the proposed model and, accordingly, our results is the assumption about the identity of all physical parameters of thermoelectric elements and thermal resistances of soldered joints between thermoelements and substrate. In addition, the validity of model results should be confirmed by experimental studies that could add certain adjustments. The advancement of a given direction is to analyze reliability indicators for thermoelectric coolers exposed to integrated impacts of mechanical, climatic, energy factors under dynamic modes, which is typical for on-board control systems.

7. Conclusions

1. Our study of the dynamic model of cooling thermoelement operation has shown the possibility of optimal control

over the thermal mode of a single-cascade TCD, taking into consideration the influence of structural and parametric factors.

2. Analytical expressions have been derived to determine the basic parameters of reliability indicators at the predefined dynamics in the functioning of a single-cascade TCD over a wide range of temperature differences and current modes of operation.

3. The results of the research make it possible to design single-cascade TCD at the assigned dynamics of functioning and to predict the basic parameters and reliability indicators over any time period.

References

1. Eslami, M., Tajeddini, F., Etaati, N. (2018). Thermal analysis and optimization of a system for water harvesting from humid air using thermoelectric coolers. Energy Conversion and Management, 174, 417–429. doi: https://doi.org/10.1016/j.enconman.2018.08.045
2. Bakhtiaryfard, L., Chen, Y. S. (2014). Design and Analysis of a Thermoelectric Module to Improve the Operational Life. Advances in Mechanical Engineering, 7 (1), 152419. doi: https://doi.org/10.1155/2014/152419
3. Choi, H.-S., Seo, W.-S., Choi, D.-K. (2011). Prediction of reliability on thermoelectric module through accelerated life test and Physics-of-failure. Electronic Materials Letters, 7 (3), 271–275. doi: https://doi.org/10.1007/s13391-011-0917-x
4. Kim, H. S., Wang, T., Liu, W., Ren, Z. (2016). Engineering Thermal Conductivity for Balancing Between Reliability and Performance of Bulk Thermoelectric Generators. Advanced Functional Materials, 26 (21), 3678–3686. doi: https://doi.org/10.1002/adfm.201600128
5. Erturun, U., Mossi, K. (2012). A Feasibility Investigation on Improving Structural Integrity of Thermoelectric Modules With Varying Geometry. Volume 2: Mechanics and Behavior of Active Materials; Integrated System Design and Implementation; Bio-Inspired Materials and Systems; Energy Harvesting. doi: https://doi.org/10.1115/smasis2012-8247
6. Song, H., Song, K., Gao, C. (2019). Temperature and thermal stress around an elliptic functional defect in a thermoelectric material. Mechanics of Materials, 130, 58–64. doi: https://doi.org/10.1016/j.mechmat.2019.01.008
7. Karri, N. K., Mo, C. (2018). Structural Reliability Evaluation of Thermoelectric Generator Modules: Influence of End Conditions, Leg Geometry, Metallization, and Processing Temperatures. Journal of Electronic Materials, 47 (10), 6101–6120. doi: https://doi.org/10.1007/s11664-018-6505-1
8. Fang, E., Wu, X., Yu, Y., Xiu, J. (2017). Numerical modeling of the thermoelectric cooler with a complementary equation for heat circulation in air gaps. Open Physics, 15 (1), 27–34. doi: https://doi.org/10.1515/phys-2017-0004
9. Mativo, J., Hallinan, K. (2019). Development of Compliant Thermoelectric Generators (TEGs) in Aerospace Applications Using Topology Optimization. Energy Harvesting and Systems, 4 (2), 87–105. doi: https://doi.org/10.1515/ehs-2016-0017
10. Manikandan, S., Kaushik, S. C., Yang, R. (2017). Modified pulse operation of thermoelectric coolers for building cooling applications. Energy Conversion and Management, 140, 145–156. doi: https://doi.org/10.1016/j.enconman.2017.03.003
11. Zaykov, V., Mescheryakov, V., Zhuravlov, Y. (2017). Analysis of the possibility to control the inertia of the thermoelectric cooler. Eastern-European Journal of Enterprise Technologies, 6 (8 (90)), 17–24. doi: https://doi.org/10.15587/1729-4061.2017.116005
12. Zaykov, V., Mescheryakov, V., Zhuravlov, Y. (2018). Analysis of relationship between the dynamics of a thermoelectric cooler and its design and modes of operation. Eastern-European Journal of Enterprise Technologies, 1 (8 (91)), 12–24. doi: https://doi.org/10.15587/1729-4061.2018.123891
13. Zaykov, V., Mescheryakov, V., Zhuravlov, Y. (2019). Influence of the mean volumetric temperature of a thermoelement on reliability indicators and the dynamics of a cooler. Eastern-European Journal of Enterprise Technologies, 1 (8 (97)), 36–42. doi: https://doi.org/10.15587/1729-4061.2019.154991
14. Zaykov, V., Mescheryakov, V., Zhuravlov, Y., Mescheryakov, D. (2018). Analysis of dynamics and prediction of reliability indicators of a cooling thermoelement with the predefined geometry of branches. Eastern-European Journal of Enterprise Technologies, 5 (8 (95)), 41–51. doi: https://doi.org/10.15587/1729-4061.2018.123890